

## Structural, magnetic and phase identification of Fe Oxide nanoparticles

S. Akbar<sup>1</sup>, \*S. F. Shaukat<sup>2</sup>, M. Nadeem<sup>3</sup>, M. S. Awan<sup>4</sup>, R. Farooq<sup>5</sup>, M. Farooq<sup>6</sup>,  
Raja J. Amjad<sup>2</sup> and Majid Niaz Akhtar<sup>2</sup>

<sup>1</sup>Department of Physics, Quaid-i-Azam University Islamabad, Pakistan.

<sup>2</sup>Department of Physics, COMSATS Institute of Information Technology, Lahore, Pakistan.

<sup>3</sup>Pakistan Institute of Nuclear Sciences and Technology, Nilore, Islamabad, Pakistan.

<sup>4</sup>Ibnsina Institute of Technology (ISIT), Islamabad, 44000, Pakistan

<sup>5</sup>Department of Chemical Engineering, COMSATS Institute of Information Technology, Lahore, Pakistan.

<sup>6</sup>Institute of Chemical Engineering and Technology, University of the Punjab, Lahore-Pakistan

### Abstract

A modified sol-gel method was introduced for the synthesis of Fe<sub>2</sub>O<sub>3</sub> nanoparticles. Different sizes (22-56 nm) of pure alpha phase (hematite) as well as an admixture of alpha (hematite) and gamma (maghemite) phases were obtained. The X-ray diffraction, Mössbauer spectroscopy and VSM magnetic measurements were carried out to verify and calculate the relative percentage of phases present in the samples. Two major size and phase controlling parameters have been identified. First, the annealing temperature affects the relative fractions of the two phases and consequently the magnetization of the particles. As annealing temperature increases; the average size of particle decreases and the coercivity of particles increases. Second, controlling parameter is molarity of the ligand agent which has been proved as inversely proportional to the size of the nanoparticles.

**Key words:** Nanoparticles, Iron oxide, Sol-gel, XRD, VSM, Mössbauer spectroscopy

\* Corresponding author: S F Shaukat, saleem@ciitlahore.edu.pk

Phone: +92-42-111-001-007, Fax: +92-42-99203100

### 1. Introduction

Fe<sub>2</sub>O<sub>3</sub> exist in four polymorph forms (alpha, beta, gamma, epsilon). Alpha has hexagonal corundum structure with mineral name whereas gamma has cubic spinel structure and found in nature as hematite and maghemite minerals respectively. The other two polymorphs, beta has cubic bixbyite structure and epsilon has orthorhombic structure. Gamma and epsilon type Fe<sub>2</sub>O<sub>3</sub> are ferromagnetic; alpha Fe<sub>2</sub>O<sub>3</sub> is a canted antiferromagnetic while beta type Fe<sub>2</sub>O<sub>3</sub> is a paramagnetic material.

The magnetic moment of bulk gamma type Fe<sub>2</sub>O<sub>3</sub> is ~430 emu/cc at room temperature while the magnetic moment of alpha type Fe<sub>2</sub>O<sub>3</sub> is very small (~1emu/cc) as compared to the gamma phase. The observed weak ferromagnetism arises from the canting of the antiferromagnetically aligned spins above TM and this spin-canting angle is  $\approx 5^\circ$  [1-4].

Hematite is potentially important in many environmental processes such as adsorption, co-precipitation, redox reactions, and dissolution. Adsorption, nanobio interactions as well as

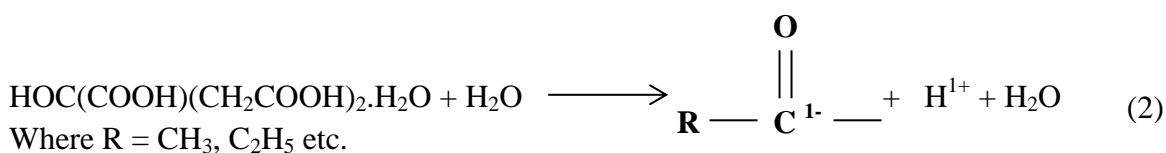
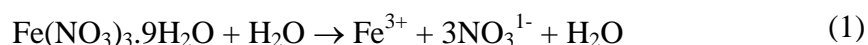
thermodynamic modelling of hematite ( $\alpha$ -Fe<sub>2</sub>O<sub>3</sub>) nanoparticle are the point of great interest from the applications point of view [5-7].

Our objective was to prepare nanosize particles of hematite ( $\alpha$ -Fe<sub>2</sub>O<sub>3</sub>) by the sol-gel method and to identify the parameters that control their size. Matijevic and Scheiner synthesized hematite particles by dissolving ferric salts in the hydrochloric acid and heating at 100°C [8]. These particles have been prepared in this research with a modified and much simpler method.

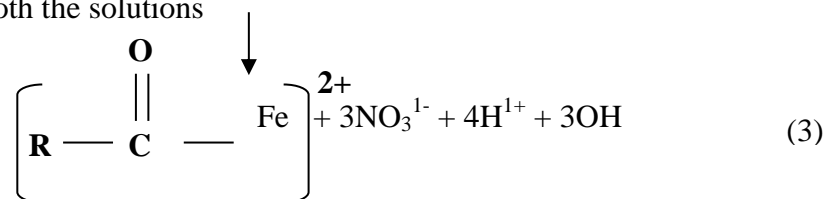
## 2. Experiments

In the present work the reagents were obtained from Aldrich: Ferric Nitrate Fe (NO<sub>3</sub>)<sub>3</sub>. 9H<sub>2</sub>O and citric acid mono hydrate up to 98% purity. Distilled water was used for solution preparation.

The 0.1M solutions of ferric nitrate and citric acid were prepared and mixed in 1:4, respectively. The iron solution was added to the citric acid solution drop wise at room temperature with vigorous stirring using a magnetic stirrer. Afterwards, the mixture was heated to a temperature of 60-70 °C, while maintaining the stirring until the gel was formed. The reaction scheme is presented below,



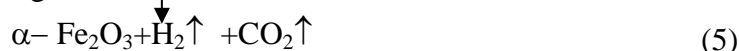
On mixing both the solutions



Gelation ↓ -H<sub>2</sub>O



On annealing the gel



The gel was put in a muffle furnace for annealing in air at a certain temperature. Typical yield of the process was 1.6g/L of pure  $\alpha$ - Fe<sub>2</sub>O<sub>3</sub> or the

admixture of  $\alpha$ - Fe<sub>2</sub>O<sub>3</sub> and  $\gamma$ -Fe<sub>2</sub>O<sub>3</sub> depending upon the synthesis conditions.

The effect of intrinsic and extrinsic parameters on the formation of iron oxide nanoparticles was studied.

For intrinsic parameter, the molarity of citric acid was varied (0.05 – 0.2M), whereas, annealing temperature was varied from 180-400 °C for extrinsic control. The details of the experimental conditions are listed in Table 1.

An X-ray diffractometer (JDX-11 Jeol) with CuK $\alpha$  was used to study the crystal structure, lattice parameter and average particle size of the

nanoparticles. A commercial vibrating sample magnetometer (VSM) was used for studying the magnetic properties at room temperature and 77K. To complement the magnetic phase identification of the nanoparticles and to calculate relative fractions of the alpha and gamma phases Mössbauer spectroscopy was performed on the samples.

**Table 1:** Experimental condition for the preparation of samples

S. no.	Citric acid solution (Molarity)	Annealing Temp. (°C)	Yield (grams)
1 to 5	0.2	180, 210, 230, 250, 400	1.6 ca
6 to 9	0.2, 0.15, 0.10, 0.05	400	1.6 ca.
10 to 12	0.2, 0.10, 0.05	250	1.6 ca.

### 3. Results and discussion

#### 3.1) XRD analysis and characterization

Two typical x-ray diffraction patterns are shown in Figure 1 representing general trends of the XRD plots obtained during the analysis. The major peaks for alpha Iron oxide are  $2\theta \cong 33.2^\circ$  and  $35.7^\circ$ , whereas,  $2\theta \cong 29.6^\circ$  and  $35.7^\circ$  are the peaks for gamma phase. For various samples belonging to the range of annealing temperature (180-250°C) have first major peak of  $33.2^\circ$  while the second major peak was at  $35.7^\circ$  (Figure1a); the relative intensity of these two major peaks exists between 70 to 80%. The other observed peaks were at  $41^\circ$ ,  $49.55^\circ$ ,  $54.25^\circ$  and  $62.55^\circ$  which

correspond to the remaining spectra of alpha phase.

The peak at  $35.7^\circ$  could be due to either of alpha or gamma phase. Relative intensities of these two major peaks and the other observed smaller peaks suggests strongly that alpha Fe<sub>2</sub>O<sub>3</sub> was the major phase in this material. The lattice constants so obtained for this set of alpha Fe<sub>2</sub>O<sub>3</sub> nanoparticles were  $a=b=5.0356 \text{ \AA}$  and  $c=13.7489 \text{ \AA}$ . However the 2<sup>nd</sup> XRD pattern was somewhat different with some of new peak and a definite change in the ratios of the two major peaks at  $33.2^\circ$  and  $35.7^\circ$  as shown in figure 1(b). While the two major peaks were still at the same positions as in figure 1 but the identities of the

highest and second highest peaks had been reversed. The peak at  $35.7^\circ$  became most intense while the  $33.2^\circ$  peak was second highest with an intensity ratio of 0.8. In the pure gamma phase the relative ratios of the two major peaks  $I_{33.2}/I_{35.7}$  is much smaller. We believe that this is an indication of both gamma and alpha phases present in the samples annealed at higher temperature. The

amount of the gamma phase is probably small and hence the smaller peaks were not so visible. Whereas, the contribution from hematite was clearly visible at  $33.2^\circ$ , it overlapped with maghemite at  $35.7^\circ$  thus leading to higher peak intensity. This pattern is confirmed decisively by the Mossbauer data discussed later.

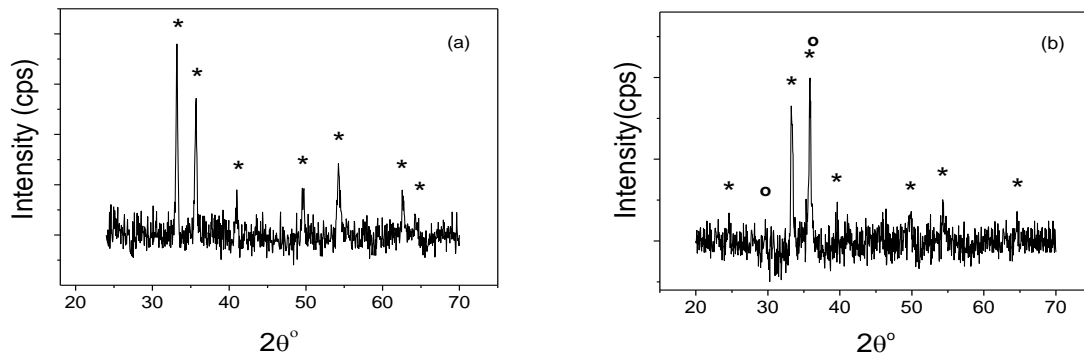


**Figure 1:**(a) XRD pattern of the sample #2, (b) sample # 8 with an average particle size of 33nm (Symbol \* and  $^{\circ}$  represents the hematite and maghemite peaks).

### 3.2) Discussion on magnetization

Magnetizations of samples were generally much higher than the expected values for the pure hematite, i.e., it should be  $\sim 0.2\text{emu/g}$  ( $1\text{emu/cc}$ ) while our values were generally in the range  $0.9\text{-}25\text{emu/g}$ , depending on different preparation parameters as shown in Table 1&2. We understand this as being due to the presence of the ferromagnetic gamma phase in small quantities in the particles. Note that it is due to the very large moment of  $\gamma\text{-Fe}_2\text{O}_3$  (about 500 times) as compared to  $\alpha\text{-Fe}_2\text{O}_3$ , a very

small amount of  $\gamma\text{-Fe}_2\text{O}_3$  was sufficient to give significant increase in moment as compared to  $\alpha\text{-Fe}_2\text{O}_3$ <sup>[9]</sup>. For example we estimated the percentage of  $\gamma\text{-Fe}_2\text{O}_3$  in the sample # 2, whose average magnetization was ( $3.66\text{emu/g}$ ), using standard values of the moments of the two phases in the bulk, i.e.,  $0.2\text{emu/g}$  for the alpha phase and  $85\text{emu/g}$  for the  $\gamma\text{-Fe}_2\text{O}_3$  phase. The average moment for a sample with  $x$  &  $1-x$ ; fractions of  $\alpha\text{-Fe}_2\text{O}_3$  and  $\gamma\text{-Fe}_2\text{O}_3$  respectively would be:

$$M_s = (x)(M_{\alpha\text{-Fe}_2\text{O}_3}) + (1-x)(M_{\gamma\text{-Fe}_2\text{O}_3})$$

Thus we estimate, using bulk values of the moments of the two phases, that sample #2 having  $M_s=3.66\text{emu/g}$  contained about 96% of  $\alpha\text{-Fe}_2\text{O}_3$  and about 4% of  $\gamma\text{-Fe}_2\text{O}_3$ . The percentage of  $\gamma\text{-Fe}_2\text{O}_3$  for one such case (sample #8,  $M_s=20.3\text{emu/g}$ ) was estimated to be about 24%. The XRD pattern for these

samples is shown in figure 1b, where the peaks corresponding to  $\gamma\text{-Fe}_2\text{O}_3$  phase are indicated. Mössbauer data on the same sample (#8) confirmed the presence of the gamma phase. Apparently the amount of  $\gamma\text{-Fe}_2\text{O}_3$  becomes detectable via x-ray diffraction.

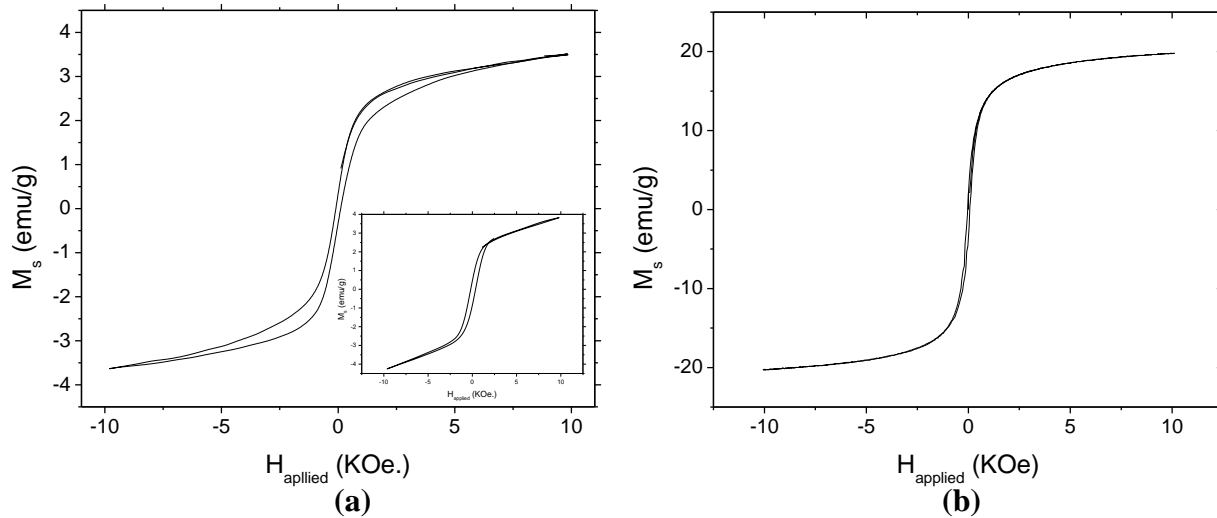


**Figure 2:** (a) M-H loop of sample #2 at 300K ( $H_c = 39\text{Oe}$ ). (Inset) M-H loop of the same sample at 77K ( $H_c = 357\text{Oe}$ ), (b) M-H loop of sample #8.

Figure 2, shows the magnetization loop of sample #2 (33nm), prepared (annealed) at 210°C and as discussed above the x-ray data shows major phase of material was hematite. This would be expected to show the weak ferromagnetism associated with this phase above Morin transition temperature, which is highly dependent on the size and morphology of particles; for bulk material it is 260K<sup>[10]</sup>. The magnetization loop shows significant hysteresis ( $H_c= 39\text{Oe}$ ), and magnetic moment of 3.66emu/g at room temperature. At 77K the moment is

slightly larger (3.72emu/g) while the coercivity increased from 39 to 357Oe. It is noticeable that the shape of the hysteresis loop is *constricted* at room temperature and becomes symmetric at 77K. Constricted loops are typically observed in materials with a mixture of a soft and hard magnetic phase. Thus at room temperature the observed response could be due to the combination of the alpha and gamma phases, the gamma phase being a soft phase with a much higher moment and the alpha phase being a hard phase having a much higher coercivity but a much lower moment. At

low temperature, on the other hand, the alpha phase is fully antiferromagnetic and the magnetization is essentially that of the gamma phase. The increase in coercivity at lower temperature could be due to the increase in the anisotropy energy of the gamma phase. It was observed that with the increase in the annealing temperature and molarity of citric acid solution the size of nanoparticles reduced; as the size reduce, surface to volume ratio increases. Hematite ( $\alpha$ -Fe<sub>2</sub>O<sub>3</sub>)-nanoparticles possess maghemite ( $\gamma$ -Fe<sub>2</sub>O<sub>3</sub>) in the near surface regions. Thus fraction of the maghemite is inversely proportion to the particle size<sup>[11]</sup>; similar trend was seen in our study. Particle size has a prominent role in the Kinetic stability and structural transformations of hematite nanoparticles.

### 3.3) Mössbauer studies

The identification of the phases and their relative proportions obtained under different preparation conditions were estimated, as discussed above, by magnetometry. These were further checked by the use of Mössbauer measurements on several representative samples. The Mössbauer data was collected using a <sup>57</sup>Co (Rh-matrix) source (initially activity of 25 mCi) in

transmission geometry. The fitting of the data was carried out using a computer code Mos90<sup>[12]</sup>. All spectra were taken at room temperature and were fitted assuming that all peaks are Lorentzian in shape.

The Mössbauer spectra for the samples #1 and #12 are given in figure 3. The parameters of the best-fitted spectra clearly indicate the presence *only* of  $\alpha$ -Fe<sub>2</sub>O<sub>3</sub>. There is no signature of  $\gamma$ -Fe<sub>2</sub>O<sub>3</sub> or any other phase. This is consistent with the magnetization measurements discussed earlier. However from the Mössbauer spectrum of samples #2 and #8 both the  $\alpha$ -Fe<sub>2</sub>O<sub>3</sub> and  $\gamma$ -Fe<sub>2</sub>O<sub>3</sub> phases could be identified. The parameters of the best-fitted spectrum and the percentage of the two identified phases for each sample are reported in Table 2. The percentage of the phases is estimated from the fractional area under the respective peaks. For sample #2 the spectrum contained two subspectra viz.  $\alpha$ -Fe<sub>2</sub>O<sub>3</sub> (84% of the total sample) and  $\gamma$ -Fe<sub>2</sub>O<sub>3</sub> (16%). In the case of sample #8 the main spectrum contained three subspectra viz.  $\alpha$ -Fe<sub>2</sub>O<sub>3</sub> (51% of the total sample);  $\gamma$ -Fe<sub>2</sub>O<sub>3</sub> (43%) and a doublet that has been identified as  $\gamma$ -FeOOH (6%).

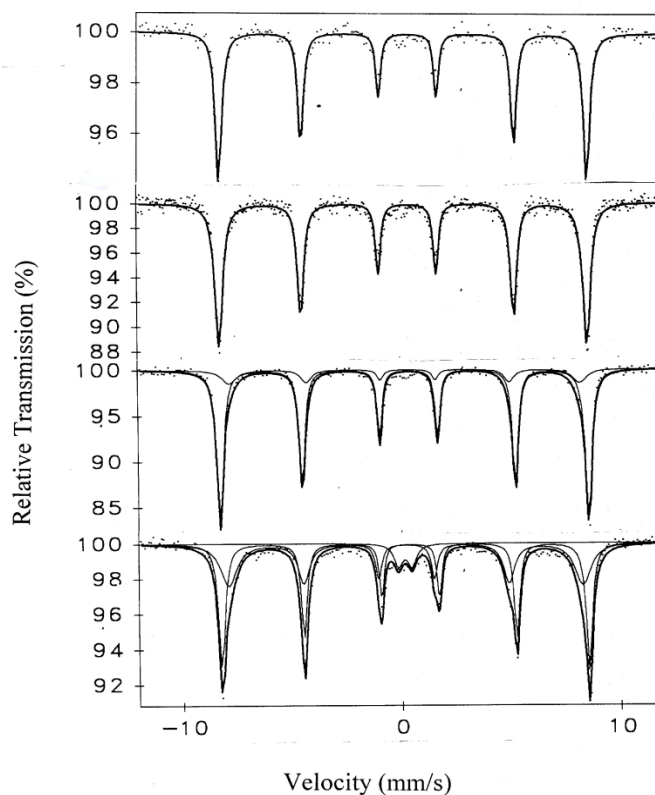


**Figure 3:** Mössbauer spectrum of samples 12, 1, 2 and 8 (from top to bottom) as discussed in the text.

**Table 2:** Mössbauer spectroscopy of different samples of nanoparticles prepared by the sol-gel method.

Sample no.	$H_{\text{eff}}$ K Oe	QS ( $\Delta$ ) mm/s	IS ( $\delta$ ) mm/s	LW ( $\Gamma$ ) mm/s	Area %	Phase
12	522	-0.213	0.37	0.35	100	$\alpha$ -Fe <sub>2</sub> O <sub>3</sub>
1	522	-0.206	0.37	0.42	100	$\alpha$ -Fe <sub>2</sub> O <sub>3</sub>
2	523	-0.209	0.37	0.35	84	$\alpha$ -Fe <sub>2</sub> O <sub>3</sub>
	498	-0.021	0.307	0.76	16	$\gamma$ -Fe <sub>2</sub> O <sub>3</sub>
8	521	-0.238	0.386	0.35	51	$\alpha$ -Fe <sub>2</sub> O <sub>3</sub>
	502	-0.03	0.308	0.88	43	$\gamma$ -Fe <sub>2</sub> O <sub>3</sub>
	**	-0.63	0.27	0.50	6	$\gamma$ -FeOOH

Mössbauer parameters: Effective magnetic field ( $H_{\text{eff}}$ ), quadrupole splitting ( $\Delta$ ), isomer shift ( $\delta$ ), line width ( $\Gamma$ ) and area under the peak.

#### 4. Conclusions

This modified sol-gel method is suitable for the preparation of pure alpha phase or an admixture of alpha, gamma phase's nanoparticles in an easier and cheaper way. Molarity of ligand (citric acid) solution and annealing temperature were identified as the size controlling parameters. Particle size has a prominent role in the Kinetic stability and structural transformations of hematite nanoparticles. The differentiation among different magnetic phases are very critical. The presence of different phases can be determined by XRD and magnetic measurements but for the calculation of exact percentages of different magnetic phases Mössbauer techniques is more reliable.

#### REFERNCES

- [1] R. Zboril, M. Mashlan, D. Petridis, 2002, *Chemistry of Materials* **14**, 969.
- [2] M J Palimi, M Rostami, et.al., 2014, *Applied Surface Science*, **320**, 60.
- [3] Gu Yi, Zhang Yong-Gang, Song Yu-Xin, Ye Hong, Cao Yuan-Ying, Li Ai-Zhen and Wang Shu-Min, 2013, *Chin. Phy. B*, **22 (3)**, 037802
- [4] R.D. Zysler, M. Vasquez-Mansilla, C. Arciprete, M. Dimitrijewits, D. Rodriguez-Sierra, C. Saragovi, J. Magn., 2001, *Magn. Mater.* **224**, 39.
- [5] Gee, S.-H. Hong, Y.-K. Sur, J.C. Erickson, D.W. Park, M.H. Jeffers and F. , 2004, *Magnetics, IEEE Transactions*, **40 (4)**, 2691.
- [6] N. Amin, S. Araj, 1987, *Phys. Rev. B*. **35**, 4810
- [7] Y. Thomas He, Jiamin Wan and Tetsu Tokunaga, 2008, *Journal of nanoparticle research*, **10 (2)**, 321
- [8] Wen Zhang, Bruce Rittmann, and Yongsheng Chen, 2011, *Environ. Sci. Technol*, **45 (6)**, 2172
- [9] Haibo Guo and Amanda S. Barnard, 2011, *J. Mater. Chem.*, **21**, 1566
- [10] Matijevic, E., Scheiner, P., J. 1978, *Colloid Interface Sci.* **63**, 509
- [11] I. V. Chernyshova, M. F. Hochella Jr and A. S. Madden, 2007, *Physical Chemistry Chemical Phys.*, **9**, 1736
- [12] Ning Shuai, Zhan Peng, Wang Wei-Peng, Li Zheng-Cao and Zhang Zheng-Jun, 2014, *Chin. Phys. B*, **23 (12)**, 127503